Electronic Supplementary Material (ESI) for Energy & Environmental Science.

Critical analysis on the quality of stability studies of perovskite and dye solar cells

Supplementary Information

1 Checklist for the implementation and reporting of an aging test

Topic	Note
Aim of the aging test	Intrinsic or extrinsic stability?
Finishing criteria of the test	Certain test duration passed, level of degradation reached, or degradation mechanism become visible?
Define test environment	Outdoor/indoor, temperature, humidity, illumination level and type, aging atmosphere? The desired illumination type is reached by selecting a suitable lamp type and possibly also a UV filter. All UV filters transmit some UV irradiation and therefore, in case of solar cells that are very sensitive to UV irradiation, the aging result might vary between pure visible (e.g. LED) and filtered UV-containing illumination. Thus, the presence of a UV filter should be reported. Report numerical values for environmental conditions, in particular avoid 'ambient' regarding humidity. Note that some environmental parameters might have greatly differing values in the aging test chamber and inside the cell: e.g., an illuminated black cell might be dozens of degrees warmer than air next to it.
Define test conditions	Open circuit, short circuit, under load, or in other electric condition? Cycling of stress factors or constant conditions?
Define measurements	Which measurements and how often are needed for reaching the aims of the aging test? Manual or automatic measurements? Check if any of the measurements is destructive or affects the condition of the cells. The measurements can also revive cells e.g. polarization can reverse degradation of charge carriers.
Design of the test cells	What kind of cells are needed for reaching the aims of the test? Possible encapsulation, the suitable reference group, total amount of cell groups? The reference group is always useful because it helps in detecting pitfalls in the experiment setup, such as insufficient encapsulation or broken measurement devices.

Analyze the nuisance factors of cell assembly and the aging test setup	Which factors could act as a nuisance? Which actions before or during the aging test could help in minimizing or removing them? Should some of the nuisance factors be followed during the aging test? Local variations in light intensity, the order of assembling the cells, and the order of measuring the cells are potential nuisance factors.
Define the ideal group size	Are you planning to use a statistical test for the result analysis or rely on comparing the means and standard deviations of the groups? What is the expected difference in the variables between the groups after the aging test? Are you targeting suggestive or decisive results? Which statistical test would fill your needs (e.g. t-test, ANOVA, ANCOVA)? Calculate the ideal group size based on the previous decisions. See Supplementary Information Section 4 for effect calculation for t-test.
Define the actual group size	Estimate how reliable your cell configuration and measurement setup are: how many extra cells should be assembled in order to have enough cells for final analysis after excluding outliers? On the other hand, how many cells you can practically assemble and age? The actual group size should be more than 1 cell in a group.
Assemble the cells	Pursue using the same material batches for all the cells and assembling all the cells within a short time period. Consider and minimize possible nuisance factors during the cell assembly, such as varying time spent for sealing the cells, air humidity, or photodegradation.
Realize the aging test	Follow the aging of the cells, especially the reference cells, in order to detect early any problems in the setup.
Measure environmental conditions during the test	Important environmental parameters, such as temperature and humidity, should be monitored frequently and at different times of day during the aging test. In case of illuminated tests, the cell temperature might differ from air temperature. Also relative humidity in the illuminated area differs from the ambient indoor humidity since the increased temperature decreases the relative humidity. The location of the temperature and humidity measurement should thus be specified when reporting the results. For illuminated tests: Measure the illumination spectrum using e.g. a spectroradiometer. Compare the intensity of UV and visible light to the AM1.5G illumination. Critical wavelength below which undesired excitations occur in the material depends on the material (see an example for TiO_2 in literature [1]) but typically, wavelengths shorter than 400nm are regarded UV. The intensity of the illumination should be followed through the aging test in case the lamps degrade. Additionally, the spatial distribution of intensity, or the intensity at each individual solar cell, should be monitored.

	The intensity could be monitored by a photodiode with sensitivity matching to the illumination spectrum. The current of the photodiode should be calibrated under the intended illumination spectrum and intensity. After the calibration, photodiode current can be used for the further monitoring of the intensity.
Analyze the test results	Is the behavior of the reference similar to the literature and your own previous tests? If not, determine the reason for the difference and whether it affects reaching the aims of the aging test. Check if the data contains significant outliers (manually, or by statistical methods such as Peirce's criterion). Determine the reasons for the abnormal data (such as a damaged cell or wrong measurement settings) and drop the cells/data from the final analysis if necessary. In case that no clear reason for the deviation is not found, drop the cells/data only with great care because the atypical results might not be outliers but represent the variation in the results that is just larger than you expected. The results could be handled with statistical tests or mean - standard deviation combination. If necessary, compensate nuisance factors by statistical methods (e.g. regression analysis or ANCOVA), otherwise e.g. t-test or ANOVA are good choices for statistical testing. Consider the practical consequences of the findings. Did the tested cell groups perform in a practically similar way? Or are the differences notable in practice?
Report the test results	Present the data of all the cells and environmental parameters that have been measured. Report also the possible outliers. The information could be placed in the supplementary information section if the data is lengthy.

2 Air humidity measurement

Indoor air humidity presented in Fig. 1 varies between 9% and 36% during one spring week in Finland, the variations being correlated with the outdoor air humidity and the time of the day (i.e., the level of air conditioning). The seasonal variations affect even more. For this location at rather constant indoor temperature, the air humidity can exceed 60% during the summer months for weeks and decrease below 20% in the winter time for long periods.

The indoor humidity data was measured in April 2017 with in-house-built automatic equipment that utilized a relative humidity module HM1500LF. The measurements were made in a modern office-laboratory building that has an air conditioning system and, due to that, rather stable indoor temperature. The outdoor air humidity data was retrieved from a weather station within 2km from the office building. The data was provided by Finnish Meteorological Institute.

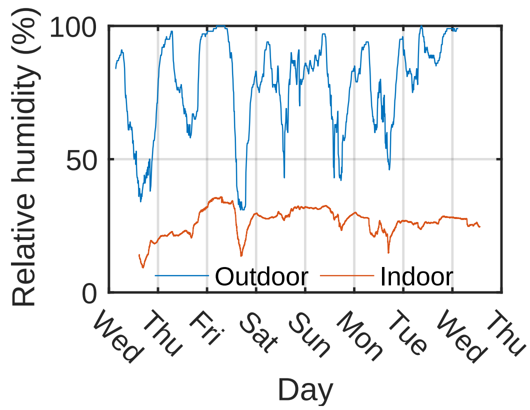

Figure 1: Relative outdoor and indoor air humidity during one spring week in a modern office-laboratory building with air conditioning.

3 Example about the evolution of electrochemical impedance spectroscopy result during the aging of the cell

The electrochemical impedance spectroscopy (EIS) results in Fig. 2 are shown as an example of how the measurement data from too degraded solar cells might be difficult to interpret. EIS is measured to acquire detailed information about the resistance and capacitance of the components of the cell [2]. Shortly, in the case that the time constants of the solar cell components (in this example counter electrode, photoelectrode, and electrolyte) are different enough, the components appear in the Nyquist plot as separated arcs, the width of the arc representing the resistance arising from the corresponding cell component (e.g., EIS data "Fresh" in Fig. 2).

Data "Aged" in Fig. 2 is from a solar cell that has started to degrade. The interpretation of the data is that the radii of the arcs on left and right side (in this case corresponding to the interface between the electrolyte and counter electrode, and the diffusion resistance of the electrolyte, respectively) have increased because of the loss of charge carriers from the electrolyte. The increased total resistance of the cell suppresses also the performance of the cell. In the case of data "Too aged" in Fig. 2, the same cell has become too degraded for reliable analysis: The arcs in Nyquist plot and the peaks in the impedance spectrum have merged together, one arc dominates the entire spectrum, and hysteresis has increased. It is clear that the overall cell resistance has increased leading to the decreased performance of the cell but at this stage the individual cell components cannot be distinguished from each other. Therefore, one can not anymore determine which components of the cell have degraded.

EIS results presented in Fig. 2 were performed under 1 Sun illumination at open circuit voltage of a DSC with 0.4 cm^2 active area, iodine-based electrolyte with methoxypropionitrile solvent, N719 dye, and a black tape mask (the dimensions of the aperture were 1 mm larger than the dimensions of the active area of the cell). The measurements were performed as fresh, after 365 hours of aging, and after 1200 hours of aging under illumination (visible and UV light intensity that corresponded to 100% and 20% of the intensity at the corresponding part of the spectrum in AM1.5G, respectively) at open circuit (additionally, IV curve and EIS measurements roughly in every 5 hours). EIS was

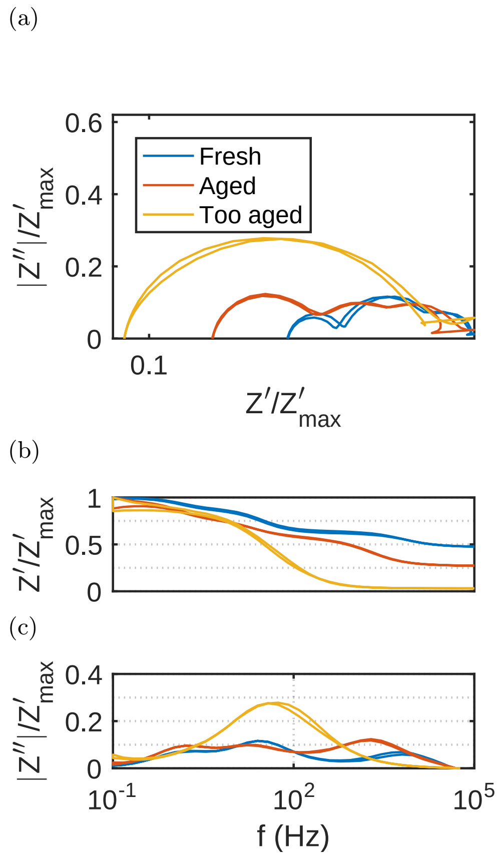

Figure 2: Electrochemical impedance spectroscopy performed under illumination at open circuit voltage of a dye solar cell as fresh (Fresh) and after 365 hours (Aged) or 1200 hours (Too aged) of aging under visible+UV light. Real (Z') and imaginary (Z'') parts of impedance are shown normalized in order to fit curves with drastically different scales to the same figure. Both a) Nyquist plot and b)-c) impedance spectra are shown.

measured with a Zahner Zennium potentiostat by sweeping frequency range $10^{-1} - 10^{5}$ Hz back and forth with 10 mV amplitude. The illumination during the measurements corresponded to 100% and 20% of the visible and UV light intensity of AM1.5G spectrum, respectively) and was calibrated using an official calibration solar cell with a KG5 colorglass filter (PV Measurements, Inc.). Nyquist plots are shown normalized in order to fit the curves with drastically different scales to the same figure. The widths of fresh, 365 hours aged, and 1200 hours aged curves are 32Ω, 58Ω, and 551Ω, respectively.

4 Calculation of the statistical power of a two-tailed independent samples t-test

In this section the standard calculation of a two tailed independent samples t-test is presented, false positive and negative errors are briefly discussed, calculation of the statistical power of two-tailed independent samples t-test is shown, and the application of power calculation for determining the sufficient group size in an solar cell aging test is presented. Finally, examples of sufficient group sizes with different parameters are presented.

4.1 Performing a t-test

A two-tailed independent samples t-test is a statistical method that is commonly used for testing if the two compared sample groups (e.g., two groups of solar cells that have both been aged) have equal or differing mean value (e.g., efficiency). The means of two independent samples, $\bar{X}_1$ and $\bar{X}_2$ with variances s_1^2 and s_2^2, respectively, are compared with each other. The number of solar cells in each sample is n_1 and n_2, respectively. The two samples are assumed to have been drawn from two normal distributions with true means of μ_1 and μ_2 and equal true variance of $\sigma^2 = \sigma_1^2 = \sigma_2^2$. In this case statistic t follows t distribution [3]:

$$t = \frac{(\bar{X}_1 - \bar{X}_2) - (\mu_1 - \mu_2)}{s_p\sqrt{\frac{1}{n_1} + \frac{1}{n_2}}} \sim T(df), \tag{1}$$

where $T(df)$ is t distribution with degrees of freedom

$$df = n_1 + n_2 - 2, \tag{2}$$

and s_p is pooled variance

$$s_p = \sqrt{\frac{(n_1 - 1)s_1^2 + (n_2 - 1)s_2^2}{df}}. \tag{3}$$

We define the null and alternative hypotheses of t-test as:

$$H_0 : \mu_1 = \mu_2 \tag{4}$$

$$H_a : \mu_1 \neq \mu_2. \tag{5}$$

By assuming that H_0 holds, statistic t simplifies to form:

$$t = \frac{\bar{X}_1 - \bar{X}_2}{s_p\sqrt{\frac{1}{n_1} + \frac{1}{n_2}}}. \tag{6}$$

Now, statistic t should follow t distribution $T(df)$ as long as H_0 holds. The more t value deviates from the central (i.e. more probable) values of $T(df)$, the more likely H_a holds instead.

A t-test is performed in practice by setting confidence level α and discarding H_0 if the probability of t statistic calculated based on the observed values, t_{obs}, belonging to distribution $T(df)$ is smaller than α. In case of two-tailed t-test, the acceptance criteria of H_0 is

$$t_l^* = t_{\alpha/2,df} < t_{obs} < t_u^* = t_{1-\alpha/2,df} \tag{7}$$

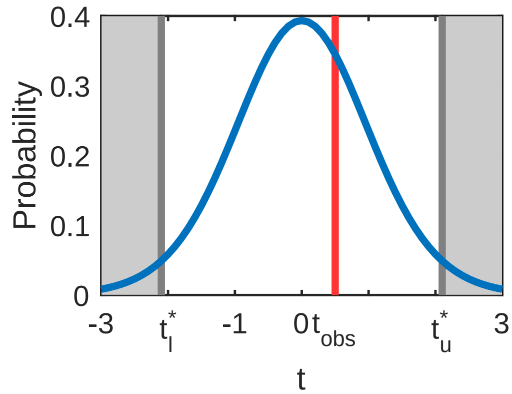

Figure 3: T distribution with rejection areas shown in grey bordered by lower and upper critical values t_l^* and t_u^*.

where t_l^* and t_u^* are called upper and lower critical values, which is illustrated in Fig. 3. The critical values are in practice either checked from a lookup table (refer to any statistics book) or calculated with the inverse cumulative distribution function of t distribution F^{-1} (e.g. function `tinv` in Matlab):

$$t_l^* = F^{-1}(\alpha/2, df), \tag{8}$$

$$t_u^* = F^{-1}(1 - \alpha/2, df). \tag{9}$$

The critical values t_l^* and t_u^* can be transformed to the space of the test variable [3]:

$$\bar{X}_l^* = t_l^* s_p \sqrt{\frac{1}{n_1} + \frac{1}{n_2}} < \bar{X}_1 - \bar{X}_2 < t_u^* s_p \sqrt{\frac{1}{n_1} + \frac{1}{n_2}} = \bar{X}_u^*. \tag{10}$$

The resulting interval with limits $\bar{X}_l^*$ and $\bar{X}_u^*$ is called a confidence interval.

4.2 Type I and II errors

There is always a possibility that a statistical test results in false deduction, either false positive result called type I error, or false negative result called type II error [4]. With hypotheses of Eqs. 4 and 5 type I error would be to deduce that the two distributions have differing means although they would be similar in reality. Correspondingly, type II error would be to deduce that the distributions are similar although they are different in reality.

Confidence level α required for performing a statistical test directly determines the probability of type I error. Type II error is determined by calculating the statistical power of the statistical test because power is the probability that type II error does not happen.

4.3 Calculating the power of a two-tailed independent samples t-test

The most common and fastest way to calculate the power of a statistical test is to use a statistical analysis software. However, understanding the principle of power calculation is beneficial for understanding how power calculation can be applied for the design of an aging test. Therefore, here

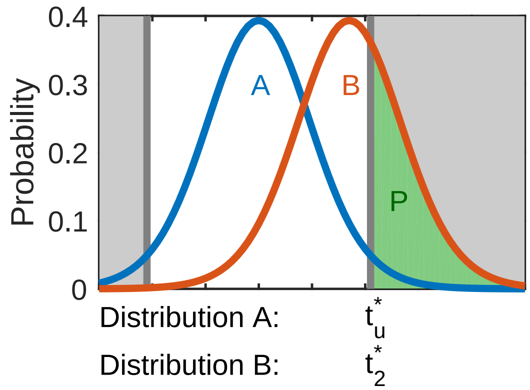

Figure 4: Principle of calculating power P. Distributions A and B are otherwise similar t distributions but shifted with each other. The upper rejection area of distribution A starts from $t = t_u^*$, and the same point in the space of distribution B is $t = t_2^*$.

the power of statistical test is calculated manually using two-tailed independent samples t-test as an example.

Let's assume that the true difference in the means between the two sample distributions defined in Section 4.1 is

$$\Delta\mu = \mu_1 - \mu_2 \neq 0. \tag{11}$$

Next, the power of the t-test is calculated in order to find out how probable it is that the difference $\Delta\mu$ is detected with t-test, resulting in the rejection of H_0 and selection of H_a instead.

Fig. 4 illustrates the basis of the calculation. Distribution A is the t distribution assumed in the t-test defined in Section 4.1, resulting from $H_0 : \mu_1 = \mu_2$. Distribution B is the true distribution (with $\Delta\mu$) that is shifted regards to distribution A. The power of the test (probability of correctly detecting $\Delta\mu$) is thus the part of distribution B that remains in the rejection area of distribution A [4], i.e. the green colored area in Fig. 4.

The border of the rejection area is t_u^* (Eq. 7) in t space of distribution A, or $\bar{X}_u^*$ (Eq. 10) in the space of the test variable. In t space of distribution B the border is critical value t_2^*. It should be noticed that t_2^* could be either the lower or upper critical value of distribution B depending on the distance between the distributions A and B: assuming that the mean of distribution B is larger than the mean of distribution A, t_2^* is the upper critical value in the case that the distance between the means of the two distributions is small, the lower critical value in the case that the distance is large. In the investigated case of Fig. 4 t_2^* is the upper critical value that is derived next.

A new t-test is defined based on Eq. 1:

$$t = \frac{(\bar{X}_1 - \bar{X}_2) - \Delta\mu}{s_p\sqrt{\frac{1}{n_1} + \frac{1}{n_2}}} \sim T(df), \tag{12}$$

$$H_{0,2} : \mu_1 - \mu_2 = \Delta\mu \tag{13}$$

$$H_{a,2} : \mu_1 = \mu_2. \tag{14}$$

Now, we can define t_2^* using Eq. 12 and $\bar{X}_u^*$ (Eq. 10):

$$t_2^* = \frac{\bar{X}_u^* - \Delta\mu}{s_p\sqrt{\frac{1}{n_1} + \frac{1}{n_2}}}. \tag{15}$$

The confidence value corresponding to t_2^* and df, α_2, is in practice determined from a lookup table or calculated from the cumulative distribution function of t distribution, F. The calculation could be done using function `tcdf` in Matlab. In the investigated case of Fig. 4 where t_2^* represents the upper critical value of distribution B:

$$1 - \alpha_2 = F(t_2^*, df). \tag{16}$$

Consequently, the power of the test (i.e., the colored area in Fig. 4) is

$$P = \alpha_2 = 1 - F(t_2^*, df) \tag{17}$$

If t_2^* would represent the lower critical value of distribution B, power of the test would be

$$P = 1 - \alpha_2 = 1 - F(t_2^*, df), \tag{18}$$

i.e., the equation is the same with respect to F in both cases.

The power of a statistical test, in this case two-tailed independent samples t-test, can be calculated after the aging test has ended and the samples have been acquired. However, it is more useful to calculate the power of the statistical test already before the aging test based on estimated values. This way, a desired power of the statistical test is reached by adjusting the number of test cells in the aging test (or improving the aging test setup so that the expected variance in the test results decreases).

4.4 Determining the sufficient test cell group size for an aging test

There are several alternative premises for determining the sufficient group size from the viewpoint of statistical analysis. Here, the sufficient number of cells is investigated from the viewpoint of optimizing the power of the statistical test selected for the result analysis. The power of a statistical test (i.e., the probability of not getting type II error) is a function of the number of the cells, the expected difference in the means of the investigated parameter (e.g. efficiency of the cells after the aging test) between the two cell groups, the expected variance, and the desired confidence level (i.e. the probability of getting type I error) of the selected statistical test. Hence, when the sufficient group size is determined via statistical power, it is actually optimized with regards of type I and II errors.

There is no simple explicit equation for the sufficient group size of a two-tailed independent samples t-test. Therefore, an implicit function is presented. It is derived from Eqs. 9, 10, 15, and 17 describing the t-test and its power, assuming group size $n1 = n2 = n$ and variance $s_1^2 = s_2^2 = s^2$:

$$\frac{(F^{-1}(1-P, 2n-2) - F^{-1}(1-\frac{\alpha}{2}, 2n-2))^2}{n} = \frac{\Delta\mu^2}{2s^2}, \tag{19}$$

where F^{-1} is the inverse probability density function of t distribution, P is power, α is confidence level, and $\Delta\mu$ is the difference between the means of the two investigated cell groups. Eq. 19 can be applied for optimizing group sizes of an aging test numerically. There are also various easy-to-use statistical analysis softwares for the calculation of sufficient sample size, e.g. G*Power.

4.5 Examples about optimal group sizes in aging tests

Here, a simple example case of determining sufficient group sizes for an aging test with two cell groups and results analysed with two-tailed independent samples t-test.The estimates for the sufficient amount of samples listed in Tables 1 were computed based on Eq. 19 using Matlab code included as additional Electronic Supplementary Information file. The imaginary example groups were designed so that they could represent efficiencies of PSCs or DSCs after an aging test.

			Estimated n	
η_1 (%)	η_2 (%)	s (%)	$P = 0.9$	$P = 0.95$
7	6	1	23	28
7	5	1	7	8
7	1	1	3	3
7	6	2.5	133	164
7	5	2.5	34	42
7	1	2.5	5	6
14	13	1	23	28
14	11	1	4	5
14	7	1	2	3
14	13	4	338	417
14	11	4	39	48
14	7	4	8	10

Table 1: Estimated sufficient group sizes for aging tests with expected post-aging efficiencies η_1 and η_2 for cell groups 1 and 2, respectively, standard deviation s for both cell groups, and statistical power P for a two-tailed independent samples t-test with confidence level 0.95. The estimations are based on the power analysis.

Table 1 demonstrates that minimizing the variations in the results arising from either cell assembly or the aging test is essential in increasing the reliability of the results. With 1% difference in the post-aging efficiencies, suppressing the standard deviations from 2.5% to 1% means that the estimated sufficient group size drops from practically impossible (>100 cells/group) to practicable (<20 cells/group), for example. It is also clear that pursuing subtle differences in the efficiency requires large cell groups whereas being able to make a statistically reliable distinction between very instable and stable cells does not require that many cells. It should be noted, however, that the computation of the sufficient group size is based on the assumption that the sample variance is equal to the population variance. If there are only a few cells in a cell group, this assumption might not be justified because there is not enough data about the true distribution of the post-aging efficiency.

5 Literature review

5.1 Selecting the investigated articles

Literature was reviewed based on the Web of Science Core Collection. Initially, the proportion of studies focusing on either stability or efficiency were estimated by searching the terms listed in Table 2 from the whole database (performed 17.6.2017).

Due to large amount of search results, the literature survey was performed on a limited group of articles: the terms in Table 3 were searched from the titles of articles published 2016. The search was repeated for year 2015 for DSCs to include more aging tests related to the topic. All the found articles were analyzed unless they did not have the full version of the article available or were unrelated to stability (e.g., were related to electron lifetimes instead of cell lifetimes). There were in total 156 articles (see the list in Supplementary Information Section 6). The acquired article group was analyzed and parameters describing the performed aging tests were listed (see the parameters in Table 4).

(TO = ((dye AND solar AND cells) OR (perovskite AND solar AND cells))) AND LANGUAGE: (English) AND DOCUMENT TYPES: (Article) Indexes=SCI-EXPANDED, SSCI, A&HCI, CPCI-S, CPCI-SSH, ESCI Timespan=All years
(TO = (((dye AND solar AND cells) AND (efficien*)) OR ((perovskite AND solar AND cells) AND (efficien*)))) AND LANGUAGE: (English) AND DOCUMENT TYPES: (Article) Indexes=SCI-EXPANDED, SSCI, A&HCI, CPCI-S, CPCI-SSH, ESCI Timespan=All years
((TO = (((dye AND solar AND cells) AND (stability OR aging OR degradation)) OR ((perovskite AND solar AND cells) AND (stability OR aging OR degradation))))) AND LANGUAGE: (English) AND DOCUMENT TYPES: (Article) Indexes=SCI-EXPANDED, SSCI, A&HCI, CPCI-S, CPCI-SSH, ESCI Timespan=All years

Table 2: Searches for Web of Science for estimating the prevalence of stability research.

dye AND solar AND cells AND	stability	OR	perovskite AND solar AND cells AND	stability
	lifetime			lifetime
	aging			aging
	degradation			degradation

Table 3: Searches for Web of Science Core Collection for the literature survey.

Many articles contained multiple aging tests, for example, storage in dark conditions and under visible illumination, that were performed on different sets of cells. In these cases, all the tests were calculated as individual tests. Similarly, if the cells had passed one aging test with stable efficiency and then were exposed to another test with very different conditions, both tests were treated individually (there were four articles with this kind of tests).

As a result, 261 tests in total were investigated. 31 of the articles did not contain aging tests of complete solar cells (either review or computational articles or contained only stability tests of materials) or were published as conference proceedings. These articles were not in the scope of this literature review. 60 of the aging tests were performed on DSCs and the rest were on PSCs.

5.2 Investigated variables

Multiple variables presented in Table 4 were determined from the investigated aging tests.

5.3 Temperature and humidity

Humidity and temperature were reported in numeric values, in humidity or temperature intervals, as being "ambient", "normal air", or "room" conditions, or not reported at all. It was rather common that the samples were stored in a glove box, and the humidity was reported but not the temperature.

5.4 Illumination level

The reported light intensity values for visible and UV illumination were divided in four categories listed in Table 4: first to numeric values (% of 1 Sun), second to quantitative intervals (% of 1 Sun), third to cases where illumination type is described but the intensity is not (>0), and fourth to cases where the illumination type or intensity is not reported.

First all the tests reporting no illumination and not showing any experimental details suggesting otherwise (such as very frequent maximum power point tracking data) were classified as dark tests. The outdoor tests were investigated as a separate group.

The reporting of light intensity varies greatly. All the studies reporting a numeric intensity for UV or visible illumination (as percentage of 1 Sun, as power density, etc.) were classified to the first group of quantitatively reported illumination. Stating the lamp type and power is not enough for reporting the intensity: even if the total power of the bulbs limits the intensity of the illumination from above, intensity dissipates to the second power of the distance between the lamp, and thus intensity actually reaching the cells remains unknown. All numeric values were transformed to percentage of 1 Sun for further analysis in the literature review, although the transform is not very accurate in all cases: when the spectrum of the illumination is unknown or when the illumination is stated as luxes. Deviations from the actual values were regarded to be small enough to serve the purpose of the literature review.

Several cases were found that the illumination was described to be 1 Sun or AM1.5G, but other experimental details (e.g., solar simulator model or the type of the lamp) suggested that the spectrum of the illumination was matched only for the visible part of the spectrum. Therefore in all the cases where the UV intensity was not specifically presented by the authors or the manufacturer of the solar simulator, UV intensity was classified to ">0". This class includes commercial solar simulators designed according to standards that do not include the UV part of the spectrum, reporting only the lamp type applied for the aging (and possibly visible intensity), as well as studies specifically reporting that the study contained or did not contain UV or visible illumination. Some solar simulator manufacturers provide example figures of the spectra of the simulator irradiation on the Internet. If these figures seemed to even roughly match the UV part of the AM1.5G irradiation, the aging tests with the specific simulator were classified to quantitatively present UV intensity (e.g. 1 Sun UV intensity if 1 Sun visible intensity was stated in the article).

Xenon, halogen, metal halide, and high pressure mercury lamps were assumed to emit UV irradiation in addition to visible irradiation, whereas LED, sulfur plasma, and high pressure sodium lamps were not. There are LEDs specifically designed for emitting UV light on the market, but here it was assumed that authors would have reported using this kind of LEDs. High pressure sodium lamps do emit minor amounts of UV, but typically the lamp cover is designed to filter UV efficiently.

In case of visible light, the fourth unknown category consisted of tests in which no illumination (or lack of illumination, using words like "stored") was mentioned in the test details but experimental information suggested that the aging test was not a dark test. These cases were infrequent. In the case of UV light, the fourth category consists of tests only mentioning that the aging test was performed under illumination, not specifying if it consisted of visible or UV light nor the simulator or lamp type utilized.

5.5 Electric state of the cells

The electric state of the cells was reported in varying ways. For most tests, the electric state was not mentioned at all. Typically, these tests were dark tests and therefore it was directly assumed that the cells had been aged at open circuit. The illuminated tests were classified to "Unknown" in the case where the electric state was not mentioned. Most of these tests are likely open circuit, judging from other experimental details presented in the articles. Some tests used repeated IV measurements as the aging condition. The test was classified to this group if IV is measured for the majority of the aging time. This is hard to define in practice because the duration of the IV measurement is often not stated. The limit was kept on average more than three measurements an hour during the tests. This would result in the cell being measured for half of the test duration, if a single IV test is assumed to take 10 minutes. We regarded this a reasonable assumption because all of the reviewed tests utilizing very frequent IV measurements were performed on PSCs that typically require slow IV measurements.

5.6 Group sizes

The number of cells in each cell group in the aging test was deduced to be one if the aging data was shown for one cell and the article text referred to the sample in singular form. Referring to the samples in plural form, although the data was shown only for one cell, was rather common. Additionally sometimes mean data with standard deviations was presented but the group size was not denoted. Both cases were classified to ">1". Sometimes the group size could not be reliably determined from the article (e.g., because of contrary choices of words) and thus the group size was classified to unknown. Additionally intervals of group sizes (e.g., 3-6 cells) were classified separately.

5.7 Aging test durations and post-aging efficiencies

The different groups in the aging tests sometimes went through different lengths of aging or different tests during the aging. The length and final efficiency of the aging test was determined based on the group that underwent the longest test, unless the shorter tests were only marginally shorter and had clearly most stable cells. If the electrodes of the cells were changed after the aging stress, the cells were classified as a separate cell group but were not taken into account when the best final efficiency in the test was determined. In the case of cycling of environmental factors, the test duration was assumed to be the duration of the whole test if the cycling included only clear stress factors (such as cycling of illumination and high temperature). If the cycling was between stress and rest (e.g., illumination and darkness at room temperature), the test duration was assumed to be the duration of the stressing circumstances (e.g., total illumination time). Outdoor tests were considered as continuous stress.

Parameter	Unit
DSC	0 or 1
PSC	0 or 1
Indoor	0 or 1
Outdoor	0 or 1
Cell	0 or 1
Panel	0 or 1
Location of study (if outdoor)	
UV-protection	0 or 1
Filtering limit if UV protection	nm or unknown
Weather protection	0 or 1
Length of aging	hours or unknown
Real time	0 or 1
Accelerated time	0 or 1
Stable or not?	$\eta_{end}/\eta_{initial}$ or unknown
Operation regime	V_{oc} or I_{sc} or load or reverse or repeated IV or unknown
Visible light	% of 1 Sun or quantitative interval or >0 or unknown
UV light	% of 1 Sun or quantitative interval or >0 or unknown
Aging temperature	°C or unknown
Aging temperature defined only as "ambient" or "room temperature"	0 or 1
Relative aging humidity	% or unknown
Aging humidity defined only as "ambient", "room humidity", or "oven humidity"	0 or 1
Water immersion	0 or 1
Cycling of stress factors	0 or 1
Amount of cells per cell group	
Data collected - IV	0 or 1
Data collected - IPCE	0 or 1
Data collected - EIS	0 or 1
Data collected - XRD	0 or 1
Data collected - other	0 or 1
Some cell measurements during the aging test, not only before and after	0 or 1
Some environment measurements during the aging test, not only once	0 or 1
Encapsulated device	0 or 1
Open device	0 or 1
ISOS was used	0 or 1
Air humidity defined only as ambient or room humidity. Or in air or in oven etc.	0 or 1
UV specifically measured by authors or manufacturer	0 or 1
Comments	

Table 4: Data collected from the investigated aging tests during he literature review.

6 Articles investigated in the literature review

1. Abdelmageed, G. *et al.* Mechanisms for light induced degradation in MAPbI3 perovskite thin films and solar cells. *Applied Physics Letters* **109,** 233905 (2016).
2. Agresti, A., Cinà, L., Pescetelli, S., Taheri, B. & Carlo, A. D. Stability of dye-sensitized solar cell under reverse bias condition: Resonance Raman spectroscopy combined with spectrally resolved analysis by transmittance and efficiency mapping. *Vibrational Spectroscopy* **84,** 106–117. ISSN: 0924-2031 (2016).
3. Agresti, A. *et al.* Efficiency and Stability Enhancement in Perovskite Solar Cells by Inserting Lithium-Neutralized Graphene Oxide as Electron Transporting Layer. *Advanced Functional Materials* **26,** 2686–2694. ISSN: 1616-3028 (2016).
4. Agresti, A. *et al.* Graphene-Perovskite Solar Cells Exceed 18% Efficiency: A Stability Study. *ChemSusChem* **9,** 2609–2619. ISSN: 1864-564X (2016).
5. Ahn, N. *et al.* Trapped charge-driven degradation of perovskite solar cells. *Nature communications* **7,** 13422 (2016).
6. Ahn, S., Jang, W., Park, J. H. & Wang, D. H. Morphology fixing agent for [6,6]-phenyl C61-butyric acid methyl ester (PC60BM) in planar-type perovskite solar cells for enhanced stability. *RSC Adv.* **6,** 51513–51519 (57 2016).
7. Akbulatov, A. F. *et al.* Hydrazinium-loaded perovskite solar cells with enhanced performance and stability. *J. Mater. Chem. A* **4,** 18378–18382 (47 2016).
8. Al-Amoudi, M. S. *et al.* Spectral studies to increase the efficiency and stability of laser dyes by charge-transfer reactions for using in solar cells: charge-transfer complexes of Ponceau S with p-chloranil, chloranilic and picric acids. *Research on Chemical Intermediates* **41,** 3089–3108 (May 2015).
9. Anitha, E. G., Vedhagiri, S. J. & Parimala, K. Conformational stability, vibrational spectra, NLO properties, NBO and thermodynamic analysis of 2-amino-5-bromo-6-methyl-4-pyrimidinol for dye sensitized solar cells by DFT methods. *Spectrochimica Acta Part A: Molecular and Biomolecular Spectroscopy* **140,** 544–562. ISSN: 1386-1425 (2015).
10. Apostolopoulou, A., Nagygyörgy, V., Madarász, J., Stathatos, E. & Pokol, G. Thermal stability and electrical studies on hybrid and composite sol–gel quasi-solid-state electrolytes for dye-sensitized solar cells. *Journal of Thermal Analysis and Calorimetry* **121,** 371–380. ISSN: 1588-2926 (July 2015).
11. Arafat Mahmud, M. *et al.* Enhanced stability of low temperature processed perovskite solar cells via augmented polaronic intensity of hole transporting layer. *physica status solidi (RRL) - Rapid Research Letters* **10,** 882–889. ISSN: 1862-6270 (2016).
12. Arora, N. *et al.* Intrinsic and Extrinsic Stability of Formamidinium Lead Bromide Perovskite Solar Cells Yielding High Photovoltage. *Nano Letters* **16.** PMID: 27776210, 7155–7162 (2016).
13. Badema, X. & Cho, K. Enhanced dye stability in dye-sensitized solar cells using 1D-structured titanate. *Journal of Industrial and Engineering Chemistry* **29,** 32–34. ISSN: 1226-086X (2015).
14. Bae, S. *et al.* Electric-Field-Induced Degradation of Methylammonium Lead Iodide Perovskite Solar Cells. *The Journal of Physical Chemistry Letters* **7.** PMID: 27462013, 3091–3096 (2016).

15. Bai, S. *et al.* Cubic: Column composite structure (NH2CH=NH2)x(CH3NH3)1-xPbI3 for efficient hole-transport material-free and insulation layer free perovskite solar cells with high stability. *Electrochimica Acta* **190,** 775–779. ISSN: 0013-4686 (2016).
16. Bai, Y. *et al.* Enhancing stability and efficiency of perovskite solar cells with crosslinkable silane-functionalized and doped fullerene. *Nature communications* **7,** 12806 (2016).
17. Baranwal, A. K. *et al.* 100 C Thermal Stability of Printable Perovskite Solar Cells Using Porous Carbon Counter Electrodes. *ChemSusChem* **9,** 2604–2608. ISSN: 1864-564X (2016).
18. Bella, F., Griffini, G., Gerosa, M., Turri, S. & Bongiovanni, R. Performance and stability improvements for dye-sensitized solar cells in the presence of luminescent coatings. *Journal of Power Sources* **283,** 195–203. ISSN: 0378-7753 (2015).
19. Bella, F. *et al.* Improving efficiency and stability of perovskite solar cells with photocurable fluoropolymers. *Science* **354,** 203–206. ISSN: 0036-8075 (2016).
20. Berhe, T. A. *et al.* Organometal halide perovskite solar cells: degradation and stability. *Energy Environ. Sci.* **9,** 323–356 (2 2016).
21. Besleaga, C. *et al.* Iodine Migration and Degradation of Perovskite Solar Cells Enhanced by Metallic Electrodes. *The Journal of Physical Chemistry Letters* **7.** PMID: 27973891, 5168–5175 (2016).
22. Bhatt, P., Kumar, M., Kant, P. C., Pandey, M. K. & Tripathi, B. Optoelectronic modelling of perovskite solar cells under humid conditions and their correlation with power losses to quantify material degradation. *Organic Electronics* **39,** 258–266. ISSN: 1566-1199 (2016).
23. Bhatt, P., Pandey, K., Yadav, P., Tripathi, B. & Kumar, M. Impedance Spectroscopic Investigation of the Degraded Dye-Sensitized Solar Cell due to Ageing. *International Journal of Photoenergy* **2016** (2016).
24. Bi, D. *et al.* High-Performance Perovskite Solar Cells with Enhanced Environmental Stability Based on Amphiphile-Modified CH3NH3PbI3. *Advanced Materials* **28,** 2910–2915. ISSN: 1521-4095 (2016).
25. Boopathi, K. M. *et al.* Synergistic improvements in stability and performance of lead iodide perovskite solar cells incorporating salt additives. *J. Mater. Chem. A* **4,** 1591–1597 (5 2016).
26. Bryant, D. *et al.* Light and oxygen induced degradation limits the operational stability of methylammonium lead triiodide perovskite solar cells. *Energy Environ. Sci.* **9,** 1655–1660 (5 2016).
27. Bush, K. A. *et al.* Thermal and Environmental Stability of Semi-Transparent Perovskite Solar Cells for Tandems Enabled by a Solution-Processed Nanoparticle Buffer Layer and Sputtered ITO Electrode. *Advanced Materials* **28,** 3937–3943. ISSN: 1521-4095 (2016).
28. Cacovich, S. *et al.* Elemental Mapping of Perovskite Solar Cells by Using Multivariate Analysis: An Insight into Degradation Processes. *ChemSusChem* **9,** 2673–2678. ISSN: 1864-564X (2016).
29. Chander, N., Khan, A. F. & Komarala, V. K. Improved stability and enhanced efficiency of dye sensitized solar cells by using europium doped yttrium vanadate down-shifting nanophosphor. *RSC Adv.* **5,** 66057–66066 (81 2015).

30. Chang, C.-Y. *et al.* Achieving high efficiency and improved stability in large-area ITO-free perovskite solar cells with thiol-functionalized self-assembled monolayers. *J. Mater. Chem. A* **4,** 7903–7913 (20 2016).

31. Chang, X. *et al.* Carbon-Based CsPbBr3 Perovskite Solar Cells: All-Ambient Processes and High Thermal Stability. *ACS Applied Materials & Interfaces* **8.** PMID: 27960426, 33649–33655 (2016).

32. Chawla, P. & Tripathi, M. Nanocomposite Polymer Electrolyte for Enhancement in Stability of Betacyanin Dye Sensitized Solar Cells. *ECS Solid State Letters* **4,** Q21–Q23 (2015).

33. Chen, H. *et al.* Extending the environmental lifetime of unpackaged perovskite solar cells through interfacial design. *J. Mater. Chem. A* **4,** 11604–11610 (30 2016).

34. Chen, P., Yin, X., Que, M., Yang, Y. & Que, W. TiO2 passivation for improved efficiency and stability of ZnO nanorods based perovskite solar cells. *RSC Adv.* **6,** 57996–58002 (63 2016).

35. Chiang, C.-H. & Wu, C.-G. Film Grain-Size Related Long-Term Stability of Inverted Perovskite Solar Cells. *ChemSusChem* **9,** 2666–2672. ISSN: 1864-564X (2016).

36. Chuang, P.-Y., Chuang, C.-N., Yu, C.-C., Wang, L.-Y. & Hsieh, K.-H. RETRACTED: Enhance the stability and efficiency of perovskite solar cell via gel-type polyurethane. *Polymer* **97,** 196–204. ISSN: 0032-3861 (2016).

37. Ciani, L., Catelani, M., Carnevale, E. A., Donati, L. & Bruzzi, M. Evaluation of the Aging Process of Dye-Sensitized Solar Cells Under Different Stress Conditions. *IEEE Transactions on Instrumentation and Measurement* **64,** 1179–1187. ISSN: 0018-9456 (May 2015).

38. Clegg, C. & Hill, I. G. Systematic study on the impact of water on the performance and stability of perovskite solar cells. *RSC Adv.* **6,** 52448–52458 (57 2016).

39. Cui, J. *et al.* Phosphor coated NiO-based planar inverted organometallic halide perovskite solar cells with enhanced efficiency and stability. *Applied Physics Letters* **109,** 171103 (2016).

40. Divitini, G. *et al.* In situ observation of heat-induced degradation of perovskite solar cells. *Nature Energy* **1,** 15012 (2016).

41. Dkhissi, Y. *et al.* Stability Comparison of Perovskite Solar Cells Based on Zinc Oxide and Titania on Polymer Substrates. *ChemSusChem* **9,** 687–695. ISSN: 1864-564X (2016).

42. Dong, Q. *et al.* Encapsulation of Perovskite Solar Cells for High Humidity Conditions. *ChemSusChem* **9,** 2597–2603. ISSN: 1864-564X (2016).

43. Dubey, A. *et al.* Solution processed pristine PDPP3T polymer as hole transport layer for efficient perovskite solar cells with slower degradation. *Solar Energy Materials and Solar Cells* **145,** 193–199. ISSN: 0927-0248 (2016).

44. Escobar, M. A. M. & Jaramillo, F. Natural Dyes Extraction, Stability and Application to Dye-Sensitized Solar Cells. *Journal of Renewable Materials* **3,** 281–291. ISSN: 2164-6325 (2015).

45. Flasque, M., Nhien, A. N. V., Moia, D., Barnes, P. R. F. & Sauvage, F. Consequences of Solid Electrolyte Interphase (SEI) Formation upon Aging on Charge-Transfer Processes in Dye-Sensitized Solar Cells. *The Journal of Physical Chemistry C* **120,** 18991–18998 (2016).

46. Garcia-Belmonte, G. & Bisquert, J. Distinction between Capacitive and Noncapacitive Hysteretic Currents in Operation and Degradation of Perovskite Solar Cells. *ACS Energy Letters* **1,** 683–688 (2016).

47. Gatti, T. *et al.* Boosting Perovskite Solar Cells Performance and Stability through Doping a Poly-3(hexylthiophene) Hole Transporting Material with Organic Functionalized Carbon Nanostructures. *Advanced Functional Materials* **26,** 7443–7453. ISSN: 1616-3028 (2016).

48. Griffini, G. *et al.* Multifunctional Luminescent Down-Shifting Fluoropolymer Coatings: A Straightforward Strategy to Improve the UV-Light Harvesting Ability and Long-Term Outdoor Stability of Organic Dye-Sensitized Solar Cells. *Advanced Energy Materials* **5.** 1401312, 1401312–n/a. ISSN: 1614-6840 (2015).

49. Guerrero, A. *et al.* Interfacial Degradation of Planar Lead Halide Perovskite Solar Cells. *ACS Nano* **10.** PMID: 26679510, 218–224 (2016).

50. Gujar, T. P. & Thelakkat, M. Highly Reproducible and Efficient Perovskite Solar Cells with Extraordinary Stability from Robust CH3NH3PbI3: Towards Large-Area Devices. *Energy Technology* **4,** 449–457. ISSN: 2194-4296 (2016).

51. Guo, Y. *et al.* Improvement of stability of ZnO/CH3NH3PbI3 bilayer by aging step for preparing high-performance perovskite solar cells under ambient conditions. *RSC Adv.* **6,** 62522–62528 (67 2016).

52. Habisreutinger, S. N., McMeekin, D. P., Snaith, H. J. & Nicholas, R. J. Research Update: Strategies for improving the stability of perovskite solar cells. *APL Materials* **4,** 091503 (2016).

53. Han, D. M., Song, H.-J., Han, C.-H. & Kim, Y. S. Enhancement of the outdoor stability of dye-sensitized solar cells by a spectrum conversion layer with 1,8-naphthalimide derivatives. *RSC Adv.* **5,** 32588–32593 (41 2015).

54. Han, Y., Pringle, J. M. & Cheng, Y.-B. Improved Efficiency and Stability of Flexible Dye Sensitized Solar Cells on ITO/PEN Substrates Using an Ionic Liquid Electrolyte. *Photochemistry and Photobiology* **91,** 315–322. ISSN: 1751-1097 (2015).

55. Högberg, D. *et al.* Liquid-Crystalline Dye-Sensitized Solar Cells: Design of Two-Dimensional Molecular Assemblies for Efficient Ion Transport and Thermal Stability. *Chemistry of Materials* **28,** 6493–6500 (2016).

56. Hou, Z. *et al.* Fabrication and stability of opened-end TiO2 nanotube arrays based dye-sensitized solar cells. *Ceramics International* **41.** The 9th Asian Meeting on Electroceramics (AMEC-9), S719–S724. ISSN: 0272-8842 (2015).

57. Ito, S. Research Update: Overview of progress about efficiency and stability on perovskite solar cells. *APL Materials* **4,** 091504 (2016).

58. Ito, S. *et al.* Light stability tests of CH3NH3PbI3 perovskite solar cells using porous carbon counter electrodes. *Phys. Chem. Chem. Phys.* **18,** 27102–27108 (39 2016).

59. Ivanou, D., Santos, R., Maçaira, J., Andrade, L. & Mendes, A. Laser assisted glass frit sealing for production large area DSCs panels. *Solar Energy* **135,** 674–681. ISSN: 0038-092X (2016).

60. Jena, A. K., Kulkarni, A., Ikegami, M. & Miyasaka, T. Steady state performance, photo-induced performance degradation and their relation to transient hysteresis in perovskite solar cells. *Journal of Power Sources* **309,** 1–10. ISSN: 0378-7753 (2016).

61. Jia, X. *et al.* Power Conversion Efficiency and Device Stability Improvement of Inverted Perovskite Solar Cells by Using a ZnO:PFN Composite Cathode Buffer Layer. *ACS Applied Materials & Interfaces* **8.** PMID: 27349330, 18410–18417 (2016).

62. Jo, J. W. *et al.* Improving Performance and Stability of Flexible Planar-Heterojunction Perovskite Solar Cells Using Polymeric Hole-Transport Material. *Advanced Functional Materials* **26,** 4464–4471. ISSN: 1616-3028 (2016).

63. Joshi, P. H. *et al.* The physics of photon induced degradation of perovskite solar cells. *AIP Advances* **6,** 115114 (2016).

64. Jung, M. *et al.* Thermal Stability of CuSCN Hole Conductor-Based Perovskite Solar Cells. *ChemSusChem* **9,** 2592–2596. ISSN: 1864-564X (2016).

65. Junhom, W. & Magaraphan, R. Co-sensitization of ZnO by CdS quantum dots in natural dye-sensitized solar cells with polymeric electrolytes to improve the cell stability. *AIP Conference Proceedings* **1664,** 140001 (2015).

66. Kim, H. M. *et al.* Edge-selectively antimony-doped graphene nanoplatelets as an outstanding counter electrode with an unusual electrochemical stability for dye-sensitized solar cells employing cobalt electrolytes. *J. Mater. Chem. A* **4,** 9029–9037 (23 2016).

67. Kim, H.-S., Seo, J.-Y. & Park, N.-G. Impact of Selective Contacts on Long-Term Stability of CH3NH3PbI3 Perovskite Solar Cells. *The Journal of Physical Chemistry C* **120,** 27840–27848 (2016).

68. Kim, H.-S., Seo, J.-Y. & Park, N.-G. Material and Device Stability in Perovskite Solar Cells. *ChemSusChem* **9,** 2528–2540. ISSN: 1864-564X (2016).

69. Kim, M.-R., Kim, J.-S., Cho, S.-E. & Lee, J.-K. Iodine Free Dye-Sensitized Solar Cells Using Nonyl Phenol Ethoxylate and Its Long-Term Stability. *Journal of Nanoelectronics and Optoelectronics* **10,** 490–493. ISSN: 1555-130X (2015).

70. Kirner, J. T. & Elliott, C. M. Are High-Potential Cobalt Tris(bipyridyl) Complexes Sufficiently Stable to Be Efficient Mediators in Dye-Sensitized Solar Cells? Synthesis, Characterization, and Stability Tests. *The Journal of Physical Chemistry C* **119,** 17502–17514 (2015).

71. Koo, B. *et al.* Pyrite-Based Bi-Functional Layer for Long-Term Stability and High-Performance of Organo-Lead Halide Perovskite Solar Cells. *Advanced Functional Materials* **26,** 5400–5407. ISSN: 1616-3028 (2016).

72. Kot, M. *et al.* Room-Temperature Atomic Layer Deposition of Al2O3: Impact on Efficiency, Stability and Surface Properties in Perovskite Solar Cells. *ChemSusChem* **9,** 3401–3406. ISSN: 1864-564X (2016).

73. Kulbak, M. *et al.* Cesium Enhances Long-Term Stability of Lead Bromide Perovskite-Based Solar Cells. *The Journal of Physical Chemistry Letters* **7.** PMID: 26700466, 167–172 (2016).

74. Kwak, C. H. *et al.* Degradation analysis of dye-sensitized solar cell module consisting of 22 unit cells for thermal stability: Raman spectroscopy study. *Solar Energy* **130,** 244–249. ISSN: 0038-092X (2016).

75. Lau, G. P. S. *et al.* Enhancing the Stability of Porphyrin Dye-Sensitized Solar Cells by Manipulation of Electrolyte Additives. *ChemSusChem* **8,** 255–259. ISSN: 1864-564X (2015).

76. Lee, S.-W. *et al.* UV degradation and recovery of perovskite solar cells. *Scientific reports* **6,** 38150 (2016).

77. Lee, Y. H. *et al.* Triphenylamine-based tri-anchoring organic dye with enhanced electron lifetime and long-term stability for dye sensitized solar cells. *Synthetic Metals* **217,** 248–255. ISSN: 0379-6779 (2016).

78. Lei, Y. *et al.* Intrinsic charge carrier dynamics and device stability of perovskite/ZnO mesostructured solar cells in moisture. *J. Mater. Chem. A* **4,** 5474–5481 (15 2016).

79. Li, B., Li, Y., Zheng, C., Gao, D. & Huang, W. Advancements in the stability of perovskite solar cells: degradation mechanisms and improvement approaches. *RSC Adv.* **6,** 38079–38091 (44 2016).

80. Li, D. *et al.* Recent progress on stability issues of organic-inorganic hybrid lead perovskite-based solar cells. *RSC Adv.* **6,** 89356–89366 (92 2016).

81. Li, W., Li, J., Niu, G. & Wang, L. Effect of cesium chloride modification on the film morphology and UV-induced stability of planar perovskite solar cells. *J. Mater. Chem. A* **4,** 11688–11695 (30 2016).

82. Li, W. *et al.* Addictive-assisted construction of all-inorganic CsSnIBr2 mesoscopic perovskite solar cells with superior thermal stability up to 473 K. *J. Mater. Chem. A* **4,** 17104–17110 (43 2016).

83. Li, W. *et al.* Enhanced UV-light stability of planar heterojunction perovskite solar cells with caesium bromide interface modification. *Energy Environ. Sci.* **9,** 490–498 (2 2016).

84. Liu, Q. *et al.* Enhanced Stability of Perovskite Solar Cells with Low-Temperature Hydrothermally Grown SnO2 Electron Transport Layers. *Advanced Functional Materials* **26,** 6069–6075. ISSN: 1616-3028 (2016).

85. Liu, Z., Sun, B., Shi, T., Tang, Z. & Liao, G. Enhanced photovoltaic performance and stability of carbon counter electrode based perovskite solar cells encapsulated by PDMS. *J. Mater. Chem. A* **4,** 10700–10709 (27 2016).

86. Lue, S. J. *et al.* Functional titanium oxide nano-particles as electron lifetime, electrical conductance enhancer, and long-term performance booster in quasi-solid-state electrolyte for dye-sensitized solar cells. *Journal of Power Sources* **274,** 1283–1291. ISSN: 0378-7753 (2015).

87. Ma, Y. *et al.* Boosting Efficiency and Stability of Perovskite Solar Cells with CdS Inserted at TiO2/Perovskite Interface. *Advanced Materials Interfaces* **3.** 1600729, 1600729–n/a. ISSN: 2196-7350 (2016).

88. Maçaira, J., Andrade, L. & Mendes, A. Laser sealed dye-sensitized solar cells: Efficiency and long term stability. *Solar Energy Materials and Solar Cells* **157,** 134–138. ISSN: 0927-0248 (2016).

89. Mahmud, M. A. *et al.* Simultaneous enhancement in stability and efficiency of low-temperature processed perovskite solar cells. *RSC Adv.* **6,** 86108–86125 (89 2016).

90. Mali, S. S. & Hong, C. K. p-i-n/n-i-p type planar hybrid structure of highly efficient perovskite solar cells towards improved air stability: synthetic strategies and the role of p-type hole transport layer (HTL) and n-type electron transport layer (ETL) metal oxides. *Nanoscale* **8,** 10528–10540 (20 2016).

91. Malinauskas, T. *et al.* Enhancing Thermal Stability and Lifetime of Solid-State Dye-Sensitized Solar Cells via Molecular Engineering of the Hole-Transporting Material Spiro-OMeTAD. *ACS Applied Materials & Interfaces* **7.** PMID: 25954820, 11107–11116 (2015).

92. Matsui, M. *et al.* Long-term stability of novel double rhodanine indoline dyes having one and two anchor carboxyl group(s) in dye-sensitized solar cells. *RSC Adv.* **6,** 33111–33119 (39 2016).

93. Matteocci, F. *et al.* Encapsulation for long-term stability enhancement of perovskite solar cells. *Nano Energy* **30,** 162–172. ISSN: 2211-2855 (2016).

94. El-Mellouhi, F., Bentria, E. T., Rashkeev, S. N., Kais, S. & Alharbi, F. H. Enhancing intrinsic stability of hybrid perovskite solar cell by strong, yet balanced, electronic coupling. *Scientific reports* **6,** 30305 (2016).

95. Mohanty, S. P. & Bhargava, P. Impact of Electrolytes Based on Different Solvents on the Long Term Stability of Dye Sensitized Solar Cells. *Electrochimica Acta* **168,** 111–115. ISSN: 0013-4686 (2015).

96. Mohanty, S. P., More, V. & Bhargava, P. Effect of aging conditions on the performance of dip coated platinum counter electrode based dye sensitized solar cells. *RSC Adv.* **5,** 18647–18654 (24 2015).

97. Moudam, O. & Gamouz, A. E. Delaying the degradation caused by water of dye-sensitized solar cells. *Organic Electronics* **36,** 7–11. ISSN: 1566-1199 (2016).

98. Nakajima, S. & Katoh, R. Mechanism of degradation of electrolyte solutions for dye-sensitized solar cells under ultraviolet light irradiation. *Chemical Physics Letters* **619,** 36–38. ISSN: 0009-2614 (2015).

99. Nie, W. *et al.* Light-activated photocurrent degradation and self-healing in perovskite solar cells. *Nature communications* **7** (2016).

100. Pascual, J. *et al.* Electron Transport Layer-Free Solar Cells Based on Perovskite-Fullerene Blend Films with Enhanced Performance and Stability. *ChemSusChem* **9,** 2679–2685. ISSN: 1864-564X (2016).

101. Pearson, A. J. *et al.* Oxygen Degradation in Mesoporous Al2O3/CH3NH3PbI3-xClx Perovskite Solar Cells: Kinetics and Mechanisms. *Advanced Energy Materials* **6.** 1600014, 1600014–n/a. ISSN: 1614-6840 (2016).

102. Peedikakkandy, L. & Bhargava, P. Recrystallization and phase stability study of cesium tin iodide for application as a hole transporter in dye sensitized solar cells. *Materials Science in Semiconductor Processing* **33,** 103–109. ISSN: 1369-8001 (2015).

103. Perumallapelli, G. R., Vasa, S. R. & Jang, J. Improved morphology and enhanced stability via solvent engineering for planar heterojunction perovskite solar cells. *Organic Electronics* **31,** 142–148. ISSN: 1566-1199 (2016).

104. Petrus, M. L. *et al.* The Influence of Water Vapor on the Stability and Processing of Hybrid Perovskite Solar Cells Made from Non-Stoichiometric Precursor Mixtures. *ChemSusChem* **9,** 2699–2707. ISSN: 1864-564X (2016).

105. Qin, C., Matsushima, T., Fujihara, T., Potscavage, W. J. & Adachi, C. Degradation Mechanisms of Solution-Processed Planar Perovskite Solar Cells: Thermally Stimulated Current Measurement for Analysis of Carrier Traps. *Advanced Materials* **28,** 466–471. ISSN: 1521-4095 (2016).

106. Ran, C., Chen, Y., Gao, W., Wang, M. & Dai, L. One-dimensional (1D) [6,6]-phenyl-C61-butyric acid methyl ester (PCBM) nanorods as an efficient additive for improving the efficiency and stability of perovskite solar cells. *J. Mater. Chem. A* **4,** 8566–8572 (22 2016).

107. Reddy, S. S. *et al.* Highly Efficient Organic Hole Transporting Materials for Perovskite and Organic Solar Cells with Long-Term Stability. *Advanced Materials* **28,** 686–693. ISSN: 1521-4095 (2016).

108. Reyna, Y. *et al.* Performance and stability of mixed FAPbI3(0.85)MAPbBr3(0.15) halide perovskite solar cells under outdoor conditions and the effect of low light irradiation. *Nano Energy* **30,** 570–579. ISSN: 2211-2855 (2016).

109. Roose, B. *et al.* Enhanced Efficiency and Stability of Perovskite Solar Cells Through Nd-Doping of Mesostructured TiO2. *Advanced Energy Materials* **6.** 1501868, 1501868–n/a. ISSN: 1614-6840 (2016).

110. Salado, M. *et al.* Extending the Lifetime of Perovskite Solar Cells using a Perfluorinated Dopant. *ChemSusChem* **9,** 2708–2714. ISSN: 1864-564X (2016).

111. Salado, M. *et al.* Interface Play between Perovskite and Hole Selective Layer on the Performance and Stability of Perovskite Solar Cells. *ACS Applied Materials & Interfaces* **8.** PMID: 27935300, 34414–34421 (2016).

112. Saliba, M. *et al.* Cesium-containing triple cation perovskite solar cells: improved stability, reproducibility and high efficiency. *Energy Environ. Sci.* **9,** 1989–1997 (6 2016).

113. Sanehira, E. M. *et al.* Influence of Electrode Interfaces on the Stability of Perovskite Solar Cells: Reduced Degradation Using MoOx/Al for Hole Collection. *ACS Energy Letters* **1,** 38–45 (2016).

114. Seidalilir, Z., Malekfar, R., Shiu, J.-W., Wu, H.-P. & Diau, E. W.-G. High-Performance Gel-Type Dye-Sensitized Solar Cells Using Poly (methyl methacrylate-co-ethylacrylate)-Based Polymer Gel Electrolyte with Superior Enduring Stability. *Journal of The Electrochemical Society* **162,** H922–H928 (2015).

115. Shahbazi, M. & Wang, H. Progress in research on the stability of organometal perovskite solar cells. *Solar Energy* **123,** 74–87. ISSN: 0038-092X (2016).

116. Shao, S. *et al.* N-type polymers as electron extraction layers in hybrid perovskite solar cells with improved ambient stability. *J. Mater. Chem. A* **4,** 2419–2426 (7 2016).

117. Si, H. *et al.* An innovative design of perovskite solar cells with Al2O3 inserting at ZnO/perovskite interface for improving the performance and stability. *Nano Energy* **22,** 223–231. ISSN: 2211-2855 (2016).

118. Singh, T., Singh, J. & Miyasaka, T. Role of Metal Oxide Electron-Transport Layer Modification on the Stability of High Performing Perovskite Solar Cells. *ChemSusChem* **9,** 2559–2566. ISSN: 1864-564X (2016).

119. Sohrabpoor, H., Puccetti, G. & Gorji, N. E. Modeling the degradation and recovery of perovskite solar cells. *RSC Adv.* **6,** 49328–49334 (55 2016).

120. Song, D. *et al.* Degradation of organometallic perovskite solar cells induced by trap states. *Applied Physics Letters* **108,** 093901 (2016).

121. Song, Z. *et al.* Perovskite Solar Cell Stability in Humid Air: Partially Reversible Phase Transitions in the PbI2-CH3NH3I-H2O System. *Advanced Energy Materials* **6.** 1600846, 1600846–n/a. ISSN: 1614-6840 (2016).

122. Soufiani, A. M. *et al.* Electro- and photoluminescence imaging as fast screening technique of the layer uniformity and device degradation in planar perovskite solar cells. *Journal of Applied Physics* **120,** 035702 (2016).

123. Stergiopoulos, T. *et al.* High boiling point solvent-based dye solar cells pass a harsh thermal ageing test. *Solar Energy Materials and Solar Cells* **144,** 457–466. ISSN: 0927-0248 (2016).

124. Suyitno, S., Saputra, T. J., Supriyanto, A. & Arifin, Z. Stability and efficiency of dye-sensitized solar cells based on papaya-leaf dye. *Spectrochimica Acta Part A: Molecular and Biomolecular Spectroscopy* **148,** 99–104. ISSN: 1386-1425 (2015).

125. Tang, Q., Zhang, L., He, B., Yu, L. & Yang, P. Cylindrical dye-sensitized solar cells with high efficiency and stability over time and incident angle. *Chem. Commun.* **52,** 3528–3531 (17 2016).

126. Tian, C. *et al.* Improved Performance and Stability of Inverted Planar Perovskite Solar Cells Using Fulleropyrrolidine Layers. *ACS Applied Materials & Interfaces* **8.** PMID: 27766845, 31426–31432 (2016).

127. Tiep, N. H., Ku, Z. & Fan, H. J. Recent Advances in Improving the Stability of Perovskite Solar Cells. *Advanced Energy Materials* **6.** 1501420, 1501420–n/a. ISSN: 1614-6840 (2016).

128. Tiihonen, A. *et al.* The effect of electrolyte purification on the performance and long-term stability of dye-sensitized solar cells. *Journal of The Electrochemical Society* **162,** H661–H670 (2015).

129. Venkatesan, S., Su, S.-C., Kao, S.-C., Teng, H. & Lee, Y.-L. Stability improvement of gel-state dye-sensitized solar cells by utilization the co-solvent effect of propionitrile/acetonitrile and 3-methoxypropionitrile/acetonitrile with poly(acrylonitrile-co-vinyl acetate). *Journal of Power Sources* **274,** 506–511. ISSN: 0378-7753 (2015).

130. Wang, D., Wright, M., Elumalai, N. K. & Uddin, A. Stability of perovskite solar cells. *Solar Energy Materials and Solar Cells* **147,** 255–275. ISSN: 0927-0248 (2016).

131. Wang, Y.-H. & Wong, D. S.-H. Modelling accelerated degradation test and shelf-life prediction of dye-sensitized solar cells with different types of solvents. *Solar Energy* **118,** 600–610. ISSN: 0038-092X (2015).

132. Wang, Y.-K. *et al.* Dopant-Free Spiro-Triphenylamine/Fluorene as Hole-Transporting Material for Perovskite Solar Cells with Enhanced Efficiency and Stability. *Advanced Functional Materials* **26,** 1375–1381. ISSN: 1616-3028 (2016).

133. Wang, Q., Chueh, C.-C., Eslamian, M. & Jen, A. K.-Y. Modulation of PEDOT:PSS pH for Efficient Inverted Perovskite Solar Cells with Reduced Potential Loss and Enhanced Stability. *ACS Applied Materials & Interfaces* **8.** PMID: 27804290, 32068–32076 (2016).

134. Wei, D. *et al.* Photo-induced degradation of lead halide perovskite solar cells caused by the hole transport layer/metal electrode interface. *J. Mater. Chem. A* **4,** 1991–1998 (5 2016).

135. Wei, J. *et al.* Suppressed hysteresis and improved stability in perovskite solar cells with conductive organic network. *Nano Energy* **26,** 139–147. ISSN: 2211-2855 (2016).

136. Xia, X. *et al.* Spray reaction prepared FA1-xCsxPbI3 solid solution as a light harvester for perovskite solar cells with improved humidity stability. *RSC Adv.* **6,** 14792–14798 (18 2016).

137. Xie, J. *et al.* Improved performance and air stability of planar perovskite solar cells via interfacial engineering using a fullerene amine interlayer. *Nano Energy* **28,** 330–337. ISSN: 2211-2855 (2016).

138. Xiong, J. *et al.* Interface degradation of perovskite solar cells and its modification using an annealing-free TiO2 {NPs} layer. *Organic Electronics* **30,** 30–35. ISSN: 1566-1199 (2016).

139. Xu, J. *et al.* Crosslinked Remote-Doped Hole-Extracting Contacts Enhance Stability under Accelerated Lifetime Testing in Perovskite Solar Cells. *Advanced Materials* **28,** 2807–2815. ISSN: 1521-4095 (2016).

140. Xu, T., Chen, L., Guo, Z. & Ma, T. Strategic improvement of the long-term stability of perovskite materials and perovskite solar cells. *Phys. Chem. Chem. Phys.* **18,** 27026–27050 (39 2016).

141. Yamamoto, K. *et al.* Degradation mechanism for planar heterojunction perovskite solar cells. *Japanese Journal of Applied Physics* **55,** 04ES07 (2016).

142. Yang, B. *et al.* Observation of Nanoscale Morphological and Structural Degradation in Perovskite Solar Cells by in Situ TEM. *ACS Applied Materials & Interfaces* **8.** PMID: 27933837, 32333–32340 (2016).

143. Yang, H. *et al.* Effect of polyelectrolyte interlayer on efficiency and stability of p-i-n perovskite solar cells. *Solar Energy* **139,** 190–198. ISSN: 0038-092X (2016).

144. Yang, W., Hao, Y., Ghamgosar, P. & Boschloo, G. Thermal Stability Study of Dye-Sensitized Solar Cells with Cobalt Bipyridyl-based Electrolytes. *Electrochimica Acta* **213,** 879–886. ISSN: 0013-4686 (2016).

145. Ye, M., Hong, X., Zhang, F. & Liu, X. Recent advancements in perovskite solar cells: flexibility, stability and large scale. *J. Mater. Chem. A* **4,** 6755–6771 (18 2016).

146. Yen, H.-J. *et al.* Large Grained Perovskite Solar Cells Derived from Single-Crystal Perovskite Powders with Enhanced Ambient Stability. *ACS Applied Materials & Interfaces* **8.** PMID: 27224963, 14513–14520 (2016).

147. Yi, Q. *et al.* High-stability Ti4+ precursor for the TiO2 compact layer of dye-sensitized solar cells. *Applied Surface Science* **356,** 587–592. ISSN: 0169-4332 (2015).

148. You, J. *et al.* Improved air stability of perovskite solar cells via solution-processed metal oxide transport layers. *Nature nanotechnology* **11,** 75–81 (2016).

149. Yue, Y. *et al.* Enhanced Stability of Perovskite Solar Cells through Corrosion-Free Pyridine Derivatives in Hole-Transporting Materials. *Advanced Materials* **28,** 10738–10743. ISSN: 1521-4095 (2016).

150. Yun, S., Lund, P. D. & Hinsch, A. Stability assessment of alternative platinum free counter electrodes for dye-sensitized solar cells. *Energy Environ. Sci.* **8,** 3495–3514 (12 2015).

151. Zhang, F., Yang, X., Cheng, M., Wang, W. & Sun, L. Boosting the efficiency and the stability of low cost perovskite solar cells by using CuPc nanorods as hole transport material and carbon as counter electrode. *Nano Energy* **20,** 108–116. ISSN: 2211-2855 (2016).

152. Zhang, H. *et al.* Pinhole-Free and Surface-Nanostructured NiOx Film by Room-Temperature Solution Process for High-Performance Flexible Perovskite Solar Cells with Good Stability and Reproducibility. *ACS Nano* **10.** PMID: 26688212, 1503–1511 (2016).

153. Zhang, Y. *et al.* Enhanced performance and light soaking stability of planar perovskite solar cells using an amine-based fullerene interfacial modifier. *J. Mater. Chem. A* **4,** 18509–18515 (47 2016).

154. Zhao, J. *et al.* Is Cu a stable electrode material in hybrid perovskite solar cells for a 30-year lifetime? *Energy Environ. Sci.* **9,** 3650–3656 (12 2016).

155. Zhu, W. *et al.* A halide exchange engineering for CH3NH3PbI3âˆ'xBrx perovskite solar cells with high performance and stability. *Nano Energy* **19,** 17–26. ISSN: 2211-2855 (2016).

156. Zhu, Z., Chueh, C.-C., Lin, F. & Jen, A. K.-Y. Enhanced Ambient Stability of Efficient Perovskite Solar Cells by Employing a Modified Fullerene Cathode Interlayer. *Advanced Science* **3.** 1600027, 1600027–n/a. ISSN: 2198-3844 (2016).

157. Zhu, Z. *et al.* Enhanced Efficiency and Stability of Inverted Perovskite Solar Cells Using Highly Crystalline SnO2 Nanocrystals as the Robust Electron-Transporting Layer. *Advanced Materials* **28,** 6478–6484. ISSN: 1521-4095 (2016).

6 Supplementary Information References

1. Tiihonen, A. *et al.* The Effect of Electrolyte Purification on the Performance and Long-Term Stability of Dye-Sensitized Solar Cells. *Journal of The Electrochemical Society* **162,** H661–H670 (2015).
2. Halme, J., Vahermaa, P., Miettunen, K. & Lund, P. Device Physics of Dye Solar Cells. *Advanced Materials* **22,** E210–E234. ISSN: 1521-4095 (2010).
3. Sheskin, D. J. *Handbook of parametric and nonparametric statistical procedures* (crc Press, 2003).
4. Winer, B. J., Brown, D. R. & Michels, K. M. *Statistical principles in experimental design* (McGraw-Hill New York, 1971).